HAL
open science

Biobased bitumen analogue formation during hydrothermal treatment of microalgae residues, part 1: Influence of reaction enthalpy on the process

Antoine Rolland, Alain Sarda, Gael Colomines, Yannick Madec, Emmanuel Chailleux, Eric Leroy

To cite this version:

Antoine Rolland, Alain Sarda, Gael Colomines, Yannick Madec, Emmanuel Chailleux, et al.. Biobased bitumen analogue formation during hydrothermal treatment of microalgae residues, part 1: Influence of reaction enthalpy on the process. Journal of Analytical and Applied Pyrolysis, 2020, 151, pp.104921. 10.1016/j.jaap.2020.104921 . hal-02962135

HAL Id: hal-02962135

https://hal.science/hal-02962135v1

Submitted on 9 Oct 2020

HAL is a multi-disciplinary open access archive for the deposit and dissemination of scientific research documents, whether they are published or not. The documents may come from teaching and research institutions in France or abroad, or from public or private research centers.

L'archive ouverte pluridisciplinaire **HAL**, est destinée au dépôt et à la diffusion de documents scientifiques de niveau recherche, publiés ou non, émanant des établissements d'enseignement et de recherche français ou étrangers, des laboratoires publics ou privés.

Biobased bitumen analogue formation during hydrothermal treatment of microalgae residues, part 1: influence of reaction enthalpy on the process.

Antoine Rolland[1], Alain Sarda[1], Gaël Colomines[1], Yannick Madec[1], Emmanuel Chailleux[2] and Eric Leroy[3,*]

1) Université de Nantes. Oniris. CNRS. GEPEA. UMR 6144. F- 44470 Carquefou. France.
2) Université Gustave Eiffel / Ifsttar / Centre de Nantes. Département MAST/ Laboratoire Matériaux pour les Infrastructures de Transports. Route de Bouaye CS4. 44344 Bouguenais. France.
3) Université de Nantes. Oniris. CNRS. GEPEA. UMR 6144. F- 44600 Saint Nazaire. France.

* corresponding author: eric.leroy@univ-nantes.fr

Abstract: The hydrothermal conversion process of industrial Spirulina sp. residues into bitumen analogue is studied with an instrumented reactor heated at 260 °C under autogenous pressure. During hydrothermal conversion experiments, an exothermic reaction starts during the heating ramp above 200 °C and perturbs the thermal regulation of the process. The end of the reaction is detected from recorded pressure and temperature signals. Thermal insulation of the reactor and monitoring of the electrical energy input for thermal regulation allows estimating a total reaction enthalpy $\Delta H_r \approx$ - 1.7 MJ/kg of dry biomass by performing two successive heating-isotherm experiments: First with biomass until complete reaction and again with reaction products after cooling. This second run is used as a reference for energy balance calculations.

Keywords: hydrothermal liquefaction. hydrothermal carbonization. microalgae. bitumen. heat of reaction.

Highlights:

- Hydrothermal conversion of Spirulina residues to bio-bitumen is exothermic.
- Thermic of the hydrothermal reactor is affected by reaction heat release.
- End of the reaction is detected by pressure and temperature signals.
- A reaction enthalpy $\Delta H_r \approx$ - 1.7 MJ/kg of dry biomass is estimated.

1 Introduction

High pressure hydrothermal treatment of biomass has been widely investigated for the fossil carbon feedstock analogues production [1]. Both most studied processes: hydrothermal carbonization (HTC) and hydrothermal liquefaction (HTL. sometimes also called thermochemical liquefaction) differ by their operating temperature and pressure range. They also allow targeting different fossil carbon products. On one hand HTC was developed for the production of solid coal like products initially from lignocellulosic biomass [1]. It typically involves temperatures ranging from 180 °C to 250 °C and autogenous pressures of approximately 2-3 MPa with residence times of 3-6 hours. On the other hand HTL is generally used to produce bio-crude oil [1] and it involves shorter treatment (few minutes to 1-2 hours), higher temperatures (280 °C to 370 °C) and pressures (10-22 MPa) taking advantage of the water subcritical properties (which becomes a solvent and a reaction media).

HTL was first applied to microalgae biomass in the 90's [2] [2]. Since this pioneering work, HTL has been widely studied for the conversion of microalgae or microalgae residues into bio oil. In a recent review, it appears that about one third of the papers dedicated to HTL treatment of biomass concern microalgae [3]. From a nature inspired point of view, HTL mimics the geological process of petroleum formation (involving lower temperatures and pressures. but over millions of years is seducing, [4] especially for microalgae which is probably the closest biomass to kerogen precursors). Besides, from an engineering and energy point of view HTL has the advantage of allowing the direct treatment of wet biomass (containing up to typically 80% moisture). In the case of microalgae that are currently produced at concentration well below 10 g/L, this avoids unreasonable energy consuming for drying before conversion [5]. Some results even suggest that for dried microalgae, HTL is more efficient than pyrolysis for bio-oil production in terms of yield and oil energy density [6].

HTC was also investigated for microalgae biomass treatment [7], allowing the production of bituminous coal like products for temperatures close to 200 °C at less than 2 MPa during less than 1 hour.

More recently, the investigation of the 240 °C to 280 °C temperature range (in between typical HTC < 250 °C and HTL > 280 °C) operating conditions for a fixed residence time of 60 min lead to the production of bitumen like products from two microalgae strain residues [8] [9]. This concept which is potentially of great interest in the context of forecast shortages of petroleum bitumen in the coming decades has been patented [10]. For both microalgae biomasses, an optimal temperature close to 260 °C leading to autogenous pressures of 5 MPa, allowed obtaining a hydrophobic phase with rheological properties mimicking those of elastomeric bio-binders, with a yield of approximately 50% compared to initial biomass. The other reaction products were mostly CO_2 in the gas phase and water soluble organic compounds [8].

These recent results suggest the scheme presented in **Figure 1**, where the temperature/pressure range between typical HTC and HTL boundaries allows targeting bio-bitumen products, instead of bio-char or bio-crude for the more conventional processing conditions of HTC and HTL, respectively. However, the thermokinetics of the process in this domain need further investigation. The purpose of the present work is to better understand these issues: The first part of the study is dedicated to the investigation of the influence of the exothermal reaction on the thermic of the process.

According to a recent review article on enthalpy change during HTC [11]**,** it can be evaluated by three different techniques : i) using the Hess law to make a balance between the energetic content of the initial biomass and the hydrothermal reaction products ii) performing DSC measurements mimicking HTC in high pressure capsules containing water and a few milligrams

of biomass [12,13] iii) making energy balance on an ad hoc thermally insulated and instrumented HTC reactor [14].

Each method has advantages and drawbacks: while not needing thermal measurements, the application of the Hess Law requires a detailed characterization of the products (gases, liquid and solid, which are highly complex in HTC/HTL) and often leads to an overestimation of the enthalpy [11]**.** DSC measurements are particularly efficient for biomasses that are homogeneous such has pure cellulose [13] but lead to high standard deviation for more complex biomasses (35% for wood [13] though recently proposed experimental procedures seem to allow reducing this measurement uncertainty [12]). For complex and non-homogeneous biomasses, the authors of the review article [11] suggest that measurements on an ad hoc HTC/HTL reactor is a better solution but that heat loss and thermal inertia issues have to be considered cautiously.

In the present work, given the complexity and composition of the spirulina biomass, this last technique will be used. For this purpose, a reactor will be equipped with an array of thermocouples to monitor the thermal field during hydrothermal conversion experiments. Then, in order to evaluate the reaction enthalpy, the reactor will be thermally insulated and the electric energy supply to the heating system will be monitored in order to allow energy balance calculations.

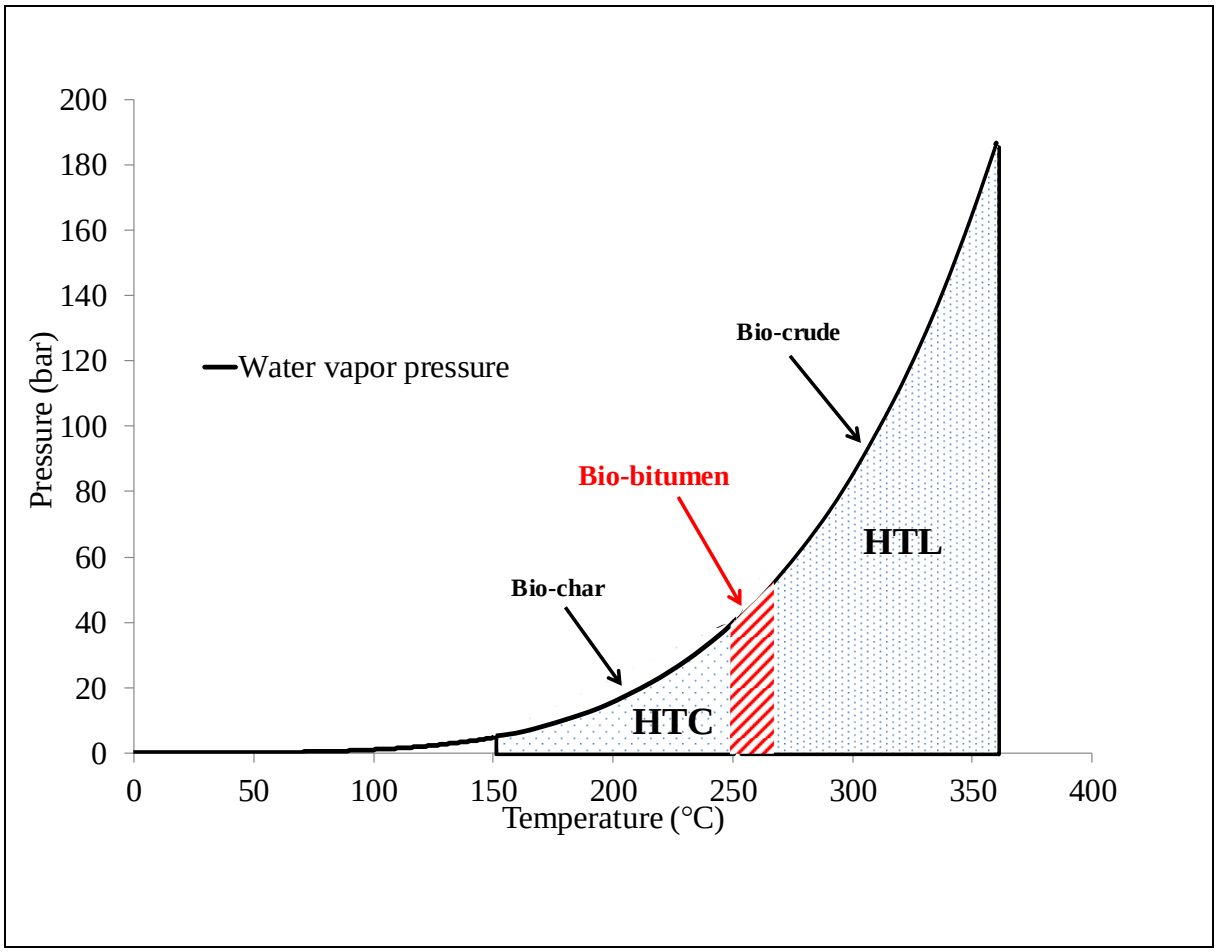

Figure 1 : Typical hydrothermal treatment conditions for the production of bio-char (HTC), bio-crude (HTL) and bio- bitumen (crossover region between HTC and HTL).

2 Materials and methods

2.1 Materials

Spirulina sp. biomass residues similar to those previously used to produce bio-bitumen [9] were supplied by AlgoSource (Alpha-Biotech. Asserac. France). This company grows Spirulina sp. and markets phycocyanin rich extracts. Depending on the season, and the harvest conditions, the algae's composition can vary. After freezing and reheating to 25 °C, the biomass is centrifuged, leading to two fractions: On one hand, an aqueous supernatant which is further purified to obtain a drinkable solution with a guaranteed phycocyanin content (0.08 wt.%); and on the other hand a solid by-product. This Spirulina sp. biomass residue was freeze dried and ball milled before hydrothermal conversion. The composition of the batch used in the present work is given in **Table 1**. The moisture content was obtained by measuring the weight loss of a 1 g sample placed in an oven at 105 °C for 1 hour. The ash content was measured by thermo-gravimetric analysis: A TGA apparatus (STA 449. Netzsch) was used to heat a 25 mg sample from 25 °C to 600 °C at 10 °C/min. under nitrogen atmosphere. The sample was then maintained at 600 °C during 1 hour under oxygen atmosphere, leading to a stable final mass corresponding to ashes residues. Procedures described in literature were used to determine the lipid [11];[12], protein [17] and carbohydrate [18] contents in the biomass. The carbon (C), hydrogen (H), nitrogen (N), and sulfur (S) content were measured using a ThermoScientific FLASH 2000 Series CHNS Analyzer (samples were heated until 980°C). The effective C. H. N and S contents in the organic phase were then calculated taking into account the ash (inorganic) content. The oxygen (O) content was estimated as the remaining fraction to reach 100% (O =100 - C – H -N -S) (**Table 1**). The heat capacity of the biomass was measured between 25°C to 80°C using a Differential Scanning calorimeter (Mettler Toledo DSC 1, TOPEM). A constant value Cp ≈ 1800 J/K/Kg. was obtained.

Table 1: Chemical composition of the Spirulina sp. residues used in this work. (Measured on freeze dried samples. (a) values in dry weight % obtained for moisture-free samples).

Component		Content (%)
Moisture		5 ±0.4
Ash[a]		8.0 ± 2.1
Protein[a]		39.1 ± 1.2
Lipid[a]		9.3 ± 1.5
Carbohydrate[a]		7.9 ± 1.2
Elemental analysis (organic phase)	C	51.5
	N	11.1
	S	1.7
	H	7.2
	O	28.5

2.2 Experiments with instrumented hydrothermal reactor

The HTL experiments were performed using a 300 mL stirred reactor with fixed head (4561 model from Parr Instrument Company. USA). For each hydrothermal conversion experiment, 45 g of Spirulina residues (dry mass 42.7 g) and 180 mL of osmosed water were introduced in the reactor at 25 °C. This corresponds to a biomass to water ratio of 0.25 (20 wt% of wet biomass). In order to remove the air still present in the reactor, nitrogen overpressure was applied 3 times and then flushed away. Then 1 bar nitrogen pressure was applied. A constant stirring rate of 100 rpm was applied during all experiments.

The experiments consisted in heating from 25 °C to 260 °C and an isotherm plateau during 400 min, followed by slow cooling. Note that such a residence time at 260°C is much longer than the 60 min. optimal conditions for bio-bitumen production described in literature [9]. Indeed, this isothermal reaction time was chosen to ensure a "complete reaction" in terms of heat released (see results and discussion sections).

Two different heating systems and thermal insulation setup were used:

- First a "standard" reactor setup (**Figure 2 (a)**) with a vessel rigid mantle heater, fitting the reactor was used for the investigation of the evolution of the temperature field in the reactor
- For the evaluation of the reaction enthalpy, a thermally insulated reactor setup (**Figure 2 (b)**) was used: a heating collar was fixed on the cylindrical surface of the reactor. In order to limit thermal losses, the bottom and cylindrical surfaces of the reactor were insulated by 5 cm thick mineral wool. Only the upper surface of the reactor steel head was left in contact with air.

Two kinds of experiments were conducted with the two setups: i) blank experiments, with the reactor containing water but no biomass. ii) real hydrothermal conversion experiments with water and Spirulina sp. biomass residues.

Additional experiments were conducted on the setup designed for reaction enthalpy evaluation: after a complete hydrothermal conversion reaction experiment, the reactor containing water and reaction products was cooled down without opening. After reaching 25 °C inside the unopened reactor, a second heating/isotherm cycle at 260 °C was performed.

In all experiments, the temperature inside the reactor was controlled using a regulation thermocouple T-R located at approximately 14.8 mm from the bottom of the reactor (**Figure 2**). During experiments, the evolution of the pressure and temperature field inside the reactor was recorded using a numerical pressure sensor (Murrelektronik. 0-200 bar) and an array of thermocouples : 8 type K stainless steel sheath (∅ 1 mm) thermocouples (T-1. T-2. T-3. T-4. T-5. T-6. T-7 and T-8) respectively located at different heights (approximately 11.8. 31.3. 44.3. 50.3. 67.3. 71.8. 81.8 and 94.8 mm from the bottom of the reactor) all on a vertical at approximately 2-3 mm. from the axis of the reactor (photo on **Figure 3**).

For the thermally insulated reactor setup, an additional thermocouple ((T-SH for “Steel Head”) was used to record the temperature of the head of the reactor (upper red part on **Figure 2(b)**) which cannot be fully insulated. In addition, the electrical energy supply (EES) to the reactor heating system was recorded: amperometric clamps (Pico Technology. France) were used to measure the electrical current intensity I(t) input into the heating collar. The electrical energy supply is thus given by:

$$EES(t) = \int_0^t U \times I(t)dt \qquad \text{Eq. (1)}$$

Where: U is the measured electrical tension.

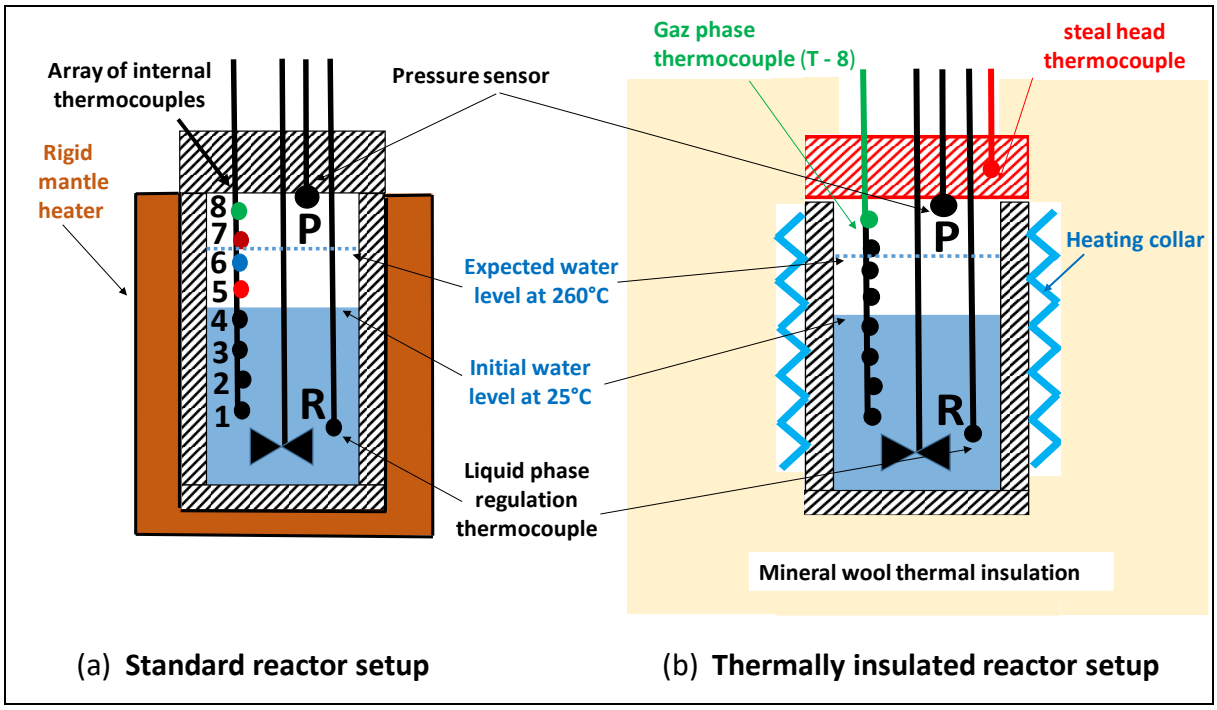

Figure 2: Instrumentation of the hydrothermal conversion reactor for the two series of experiments: (a) Standard setup for the investigation of internal thermal field and (b) thermally insulated setup for energy calculations.

Figure 3: Photo of the instrumented head (b) showing the array of thermocouples, the stirring propeller, the regulation thermocouple and the internal cooling coil.

3 Results

3.1) Temperature field inside the reactor (non-thermally insulated experiments)

Figure 4 shows the internal temperature and pressure measurements in the standard reactor setup (non-thermally insulated as shown on **Figure 2 (a)**) during experiments with only water (referred as water-only experiments in the following) and real biomass hydrothermal conversion experiments. The temperatures recorded by the thermocouples T-1, T-2, T-3 and T-4 that are below the initial water level at 25 °C were almost identical to that of the regulation thermocouple T-R indicating a homogeneous temperature of the liquid phase during the experiments. Consequently, for the sake of clarity, only one temperature T-R.1.2.3.4 was plotted on **Figure 4** (Note that the color code of the thermocouples signals is the same as in **Figure 2 (a)**)

When the reactor only contains water, the regulation thermocouple of the reactor reaches the isothermal reaction temperature of 260 °C after 60 minutes (**Figure 4(a)**). This heating time is reduced to 40 minutes in presence of the biomass (**Figure 4(b)**), with a 10 °C overshoot. This indicates the thermal regulation of the process is strongly influenced by the exothermal reaction.

The temperatures recorded by the thermocouples initially above the water level at 25 °C (T-5, T-6, T-7 and T-8) show other differences between the two experiments:

- For the water-only experiment, during the heating step, these temperatures are initially lower than that of the liquid phase (T-R.1.2.3.4). Then they successively become equal to it. For T-5 and T-6, this may be ascribed to the thermal expansion of the liquid phase in which they are immersed at 260 °C. Indeed, as a first approximation, the limit between the two phases can be estimated by considering the thermal expansion of the initial water volume:

$$h_{260°C} = h_{25°C} \times \frac{d_{25°C}}{d_{260°C}} \qquad \text{Eq. (2)}$$

Where : $h_{260°C}$ and $h_{25°C}$ are the height of water level in the reactor, and $d_{260°C}$ and $d_{25°C}$ are the densities of liquid water, equal to 1 at 25 °C and to 0.783 at 260 °C [19]**.**

This leads to an aqueous phase level at $h_{260°C}$ = 73 mm that is to say between T-6 and T-7. For T-7 and T-8, the fact that they become equal to T-R above 200 °C indicates that for water only, the temperature field inside the reactor is uniform. That is to say that the liquid and gas phases have the same temperature.

- On the contrary a heterogeneous temperature field is detected in the reactor in the presence of biomass. While the temperatures measured by the thermocouples T-5 and T-6 more or less follow T-R and become equal to it above 200 °C. T-7 and T-8 always remain significantly lower than T-R and even decrease during the isothermal reaction plateau.

The theoretical vapour pressure P_{water} was calculated using the Antoine equation:

$$P_{water} = 10^{A-\frac{B}{C+T}} \qquad \text{Eq. (3)}$$

Where: A = 8.14019; B = 1810.94 and C = 244.485 are constants [20]**.** In this equation, T is in °C and P_{water} in Torr (1 Torr = 133.322 Pa).

The plot of P_{water} as a function of time on Figure 3 assumes that T = T-R, the temperature of the liquid phase. For the water-only experiment (**Figure 4(a)**) the measured pressure signal is very close to the theoretical P_{water} curve. This indicates that the Antoine equation is a good approximation to estimate the pressure increase as a function of T-R despite the presence of nitrogen is neglected. During the isotherm, the pressure remains constant around 47 bars, the vapor pressure of water at 260 °C.

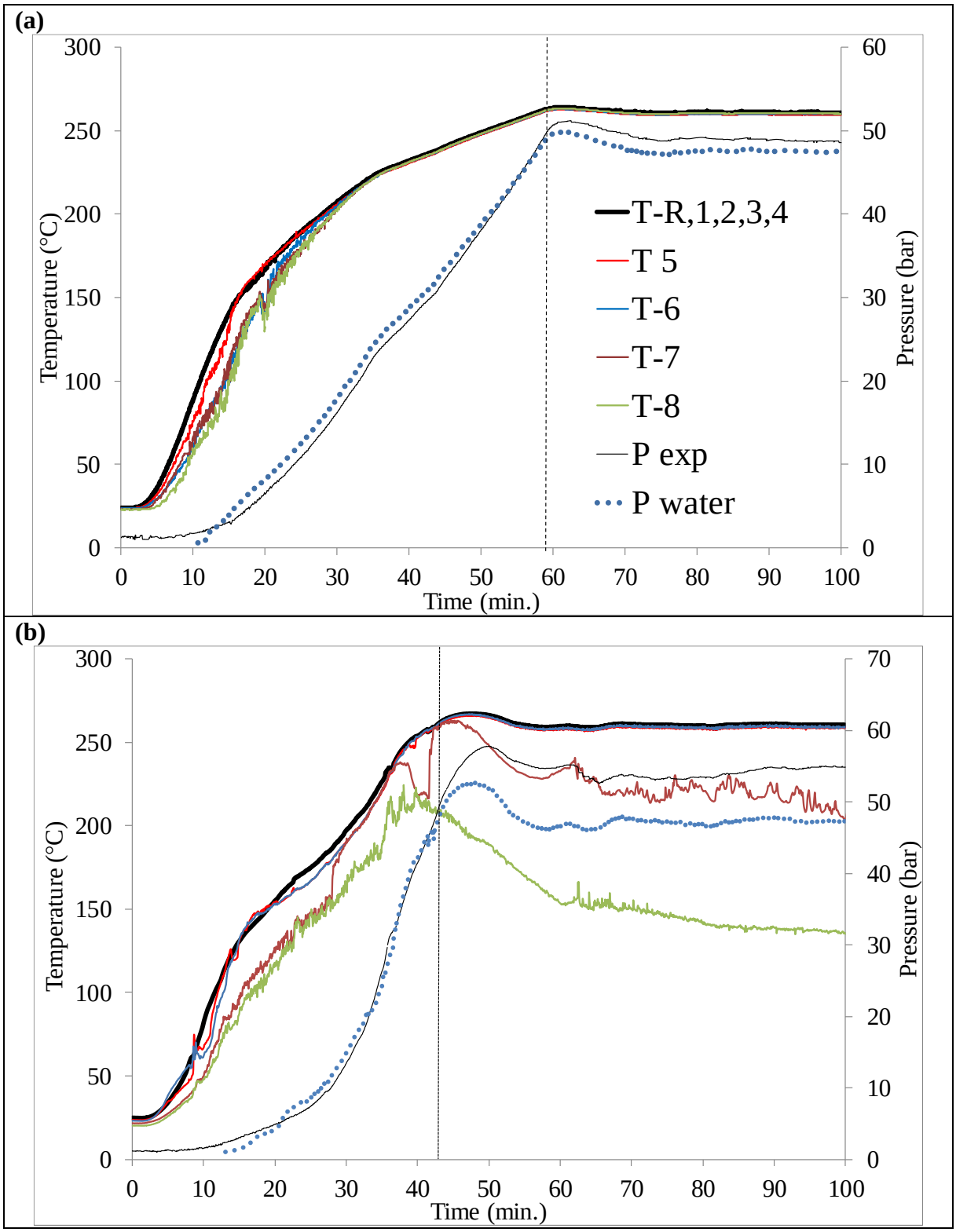

Figure 4: Temperature and pressure measurements inside the standard reactor setup during hydrothermal conversion experiments: blank experiment with water only (a) and hydrothermal conversion of industrial Spirulina sp. biomass residues (b). The color code for measured temperature and pressure signals is given on (a) and corresponds to that on Figure 2 (a)**.** The theoretical vapor pressure P_{water} curve is calculated using Eq (11).

When biomass is present (**Figure 4(b))**, the pressure inside the reactor is very close to the vapor pressure of water predicted by the Antoine equation during the heating step. However, when the isotherm is nearly reached, the measured pressure starts to increase compared to the predicted water vapor pressure. Even after the stabilisation of the regulation thermocouple's temperature (i.e. a long time after the temperature's overshoot) at 80min, it is noticeable that the pressure increases due to the release of gas products. This suggest that the pressure signal can be used to detect the end of the reaction.

3.2) *Reaction Enthalpy evaluations*

The measurements performed on the thermally insulated reactor setup (**Figure 2 (b)**) are shown on **Figure 5**. The data obtained for the three kinds of experiments described in the materials and methods section are plotted: i) an experiment with only water. ii) a hydrothermal conversion experiment with water and spirulina biomass; and iii) an experiment conducted on the unopened reactor after hydrothermal conversion and cooling to 25 °C: the reactor thus contains water and hydrothermal conversion products. Note that the same colour code as in **Figure 2 (b)** is used.

Figure 5 (a) focuses on the evolution of the internal thermal field in relation with the energy input by the heating collar: For the sake of clarity, not all temperature signals recorded inside the reactor are plotted: Only the temperature of the liquid phase (T-R in black) and the gas phase (T-8 in green) are shown. The electrical energy supply curves are plotted in blue. **Figure 5 (b)** Focuses on the internal pressure signal P (plotted in black) and the temperature of the non-thermally insulated steel head T-SH (plotted in red).

For the three experiments**,** the evolutions of T-R are similar; indicating that thermal regulation of the aqueous phase is the same. On the contrary, the evolutions of all the other signals are very different for the three experiments.

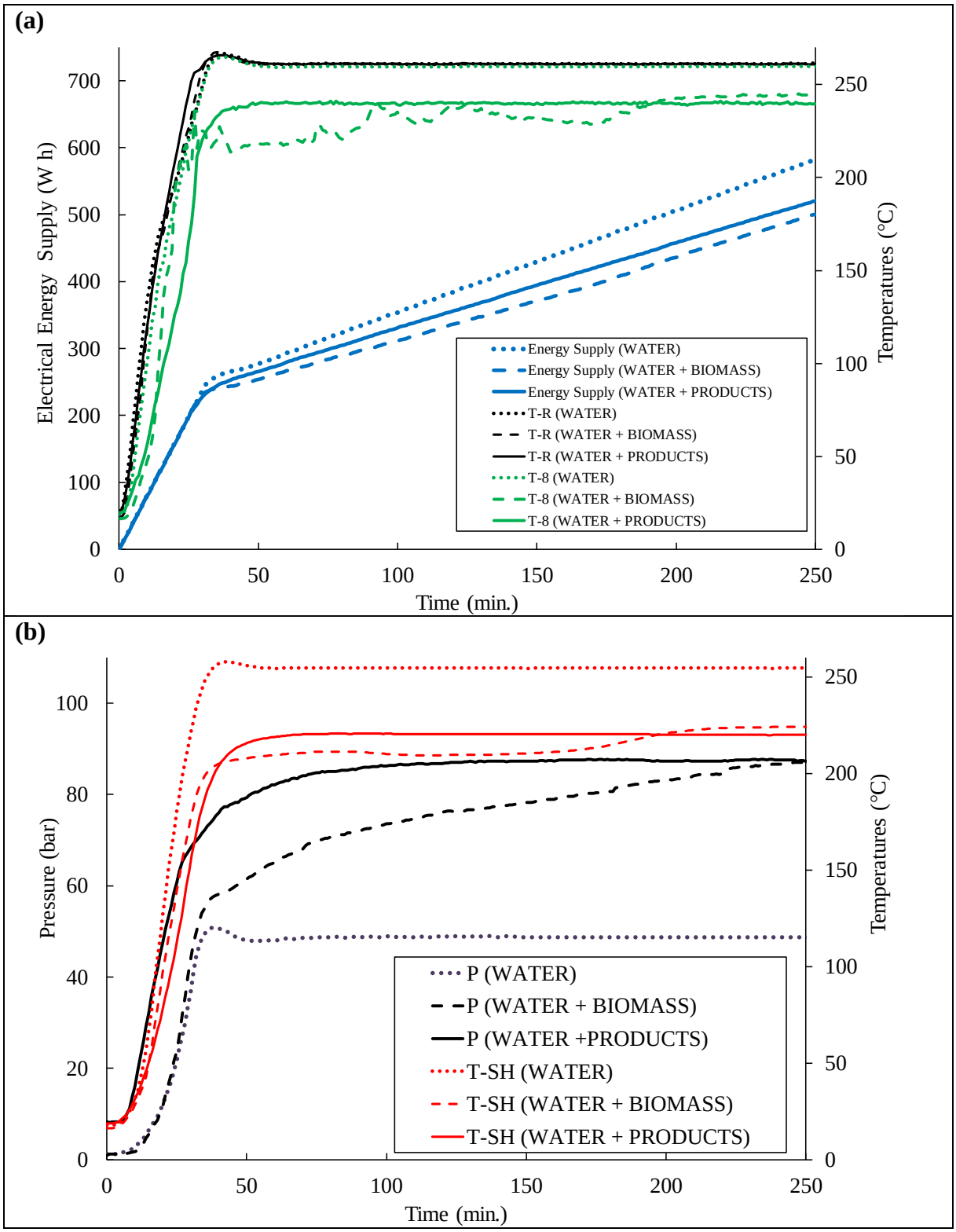

Figure 5: Temperature, pressure and energy measurements with the thermally insulated reactor setup (colour code is the same as in **Figure 2(b)**). Data for 3 experiments is plotted: i) with WATER only (dotted line). ii) with WATER + BIOMASS (dashed lines) and iii) WATER + CONVERSION PRODUCTS (solid lines).

Let's first consider the electrical energy input curves: During the heating step (from 25 °C to 260 °C), these three curves follow a similar linear trend with a slope of ≈ 475 W. This corresponds to the electrical power required for heating the reactor and its content.

Less electrical power is needed to maintain the temperature of the liquid phase at 260 °C during the isothermal step, and so lower slopes are observed. However, the fact that these slopes are positive can be ascribed to the thermal losses.

The two experiments for which no reactions are occurring show perfectly linear behaviour from 50 min till the end (420 min): The highest slope/power supply is observed for the experiment with water only with ≈ 92 W while a slope/power supply of ≈ 77 W is observed for the experiment with water and hydrothermal conversion products. These two slopes are associated to different constant values of the non-insulated steel head (T-SH = 255 °C with water and T-SH = 220 °C with water + products.) These results are consistent with a rule of thumb: the higher the temperature of the non-insulated reactor steel head, the higher the thermal loss (and so the higher the slope/power supply to maintain the isotherm). It should be pointed out that these required power supply values are much smaller than that observed for water (≈ 240 W) in the work of Merzari et al [14] on a similar ad hoc reactor for enthalpy measurements. This suggests that the thermal insulation of our experimental setup is quite efficient despite the absence of thermal insulation of the steel head.

For the hydrothermal conversion experiment with water and biomass, the behaviour of the energy supply curve during the isotherm is not linear until approximately 150 min due to the exothermal reaction. After 150 min, a linear asymptote is observed with a slope/power supply ≈ 75 W which is very close to that observed during the reheating experiment with water and hydrothermal conversion products.

These first observations suggest that the reaction's exotherm starts when the temperature reaches 260°C and ends at a certain time after 150 min. The consideration of the other signals recorded inside the reactor (**Figure 5)** allow a better estimation of this ending of the reaction:

- The gas phase temperature (T-8): As previously observed on **Figure 4**, it is lower than the liquid phase temperature (T-R) in presence of biomass. This is also the case during the reheating experiment of the reactor containing water et reaction products, for which a plateau is observed at T-8 ≈ 240°C. A similar plateau is reached during the hydrothermal conversion reaction after 200 min.
- The pressure signal (P): As previously observed on **Figure 4**, while a plateau at P ≈ 48 bar is observed during the isotherm in presence of water only, the pressure increases during the hydrothermal conversion experiment due to the production of gaseous products (mainly CO_2 according to previous studies [8]), until reaching a plateau at P ≈ 87 bar after 220 min. It is striking that the level of pressure P ≈ 87 bar is observed during the reheating experiment. It suggests that no additional gas products are formed and that the reaction ends after 220 min.

A similar trend is observed for the temperature of the reactor steel head: The T-SH curves in presence of biomass or reactions products show plateau values that are significantly lower than for the water only experiment (T-SH ≈ 255 °C). This may explain the associated lower temperature of the neighbouring gas phase, due to lower convective heat transfers from the metallic internal surfaces of the reactor. During the reactive experiment T-SH follows a three step behaviour during the T-R isotherm at 260 °C: until 150 min a roughly constant value T-SH ≈ 210 °C is observed. Then it increases to reach a second plateau after 220 min. at T-SH ≈ 224 °C (which is close to the constant value observed for the reheating experiment with water and reaction products).

Anyhow, all these observations lead to the conclusion that the reaction ends at 220 min. This information is useful for estimating the reaction enthalpy.

4) Discussion

In their recent work Merzari et al. [14] estimate the reaction enthalpy considering the experiment with water only as a baseline, assuming similar heat losses. This assumption is not true in our case, since the different slopes prove the contrary. Consequently, it necessary leads to a significant overestimation of the heat of reaction. However, we can first try applying the calculation method of Merzari et al. [14]. It is summarized by the following equation:

$$\Delta H_{rM} = \frac{E_{(water+biomass)}(t_f) - E_{(water)}(t_f) - \int_{25}^{260}(m_{biomass} \times C_{p\ biomass}) \times dT}{m_{dry\ biomass}} \qquad \text{Eq. (4)}$$

Where:

- t_f is the time of the end of the reaction. Note that in the work of Merzari et al. [14] an arbitrary shut down of power supply is imposed after 3 hours, regardless of any information about the end of the reaction. In our case t_f =220 min. will be used, since it was detected as the end of the reaction from pressure, temperature and energy supply signals.
- $E_{(water)}(t_f)$ and $E_{(water+\ biomass)}(t_f)$ are the values of the cumulative electrical energy supply measure at t_f =220 min. for the water only experiment and for the hydrothermal conversion experiment (water + biomass), respectively.
- $m_{biomass}$ is the mass of wet biomass introduced in the reactor (45 g)
- $C_{p\ biomass}$ is the heat capacity of wet biomass introduced in the reactor (assumed equal to the value of 1800 $J.K^{-1}.kg^{-1}$ measured between 25°C and 80°C)
- $m_{dry\ biomass}$ is the mass of dry biomass introduced in the reactor (42.75 g)

This leads to a total reaction enthalpy of ΔH_{rM} = -7.3 MJ/kg of dry biomass. Such an overestimated value (due to the evidence of higher heat losses for the water only experiment) is actually very close to that obtained by Merzari et al. [14] for the hydrothermal conversion of an organic fraction of municipal solid waste (OFMSW) which has a rather close elemental composition (with only a lower nitrogen and ash contents).

In order to refine the estimation of the reaction enthalpy, we propose to use the re-heating experiment curve as a baseline. This assumption seems more reasonable since we have observed that during the isotherm, the slopes corresponding to power supply are very close after the end of the reaction, indicating similar heat losses. We thus propose the following equation:

$$\Delta H_r = \frac{E_{(water+biomass)}(t_f) - E_{(water+products)}(t_f) - \int_{25}^{260}(m_{biomass} \times C_{p\ biomass}) \times dT + \int_{25}^{260}(m_{products} \times C_{p\ products}) \times dT}{m_{dry\ biomass}}$$

Eq. (5)

In this equation, new parameters appear:

- $E_{(water + products)}(t_f)$ is the value of the cumulative electrical energy supply at 220 min. for the re-heating experiment.
- $m_{products}$ is the mass of the reaction products present in the reactor
- $C_{p\ products}$ is the heat capacity of the reaction products.

As a first approximation, we assume that the difference of mass and heat capacity between initial biomass and final reaction products can be neglected:

$$m_{biomass} \times C_{p\ biomass} \approx m_{products} \times C_{p\ products} \qquad \text{Eq. (6)}$$

This assumption may lead to slight underestimation of the reaction enthalpy. Indeed, recent work on DSC measurements mimicking HTC in high pressure capsules by Pecchi et al. **[11]** suggest that such a heat capacity change between initial biomass and reaction products is not

negligible. We also neglect possible additional thermal effects related to the presence of the CO_2, which modifies internal pressure and/or may be partially water soluble at lower temperatures.

However, this leads to the following simplified expression of the reaction enthalpy:

$$\Delta H_r \approx \frac{E_{(water+biomass)}(t_f) - E_{(water+products)}(t_f)}{m_{dry\ biomass}} \qquad \text{Eq. (7)}$$

This equation leads to a hydrothermal reaction enthalpy ΔHr ≈ -1.7 MJ/kg. This value is closer to literature values obtained by DSC measurements for various biomass **[11]** [13] than that obtained with the method of Merzari et al. [14]. It is however slightly higher than for lignocellulosic biomass which is typically closer to -1 MJ/kg or lower [13]**.** The higher value for spirulina biomass may be ascribed to the presence of lipids and proteins which have more energetic content than carbohydrates.

Coming back, to the heating-isotherm experiments performed with the reactor using a vessel rigid mantle heater without thermal insulation clearly showed that this rather small enthalpy of reaction strongly affects the thermic of the process. However, this perturbation of the thermal regulation was significantly lower in the case of the thermally insulated reactor experiments. This supports the conclusion of a recent review article [11] that for the upscaling of such hydrothermal treatment, the heat recovery approach recently described [21] is probably more important than the small reaction exothermicity.

5 Conclusions

The hydrothermal conversion of industrial Spirulina sp. residues to bio-bitumen at 260 °C was studied with a thermally instrumented reactor (45 g of biomass scale). Experiments lead to the conclusion that the exothermic reaction enthalpy above 200 °C has a strong influence on heating and isothermal regulation of the process when the reactor is not thermally insulated. The reaction enthalpy $\Delta H_r \approx$ - 1.7 MJ/kg estimated by energetic measurements on the reactor in thermally insulated conditions of dry Spirulina biomass is slightly higher than the scarce values available in literature for other biomass, but may be ascribed to the composition of the Spirulina residues used.

Acknowledgments

The authors acknowledge financial support of the French National Agency for Research ANR (Algoroute project. grant ANR-16-CE08-0017) and would like to thank Mme Laurence Lavenant Ing. and Delphine Drouin for their help in biomass characterization.

Declaration of interest

None

References

[1] V. Grönberg, H. Wikberg, J. Jermakka, K. Kemppainen, M. Kleen, C. Laine, V. Paasikallio, A. Oasmaa, Hydrothermal refining of biomass: An overview and future perspectives, Tappi J. 14 (2015) 195–207.

[2] Y. Dote, S. Sawayama, S. Inoue, T. Minowa, S. Yokoyama, Recovery of liquid fuel from hydrocarbon-rich microalgae by thermochemical liquefaction, Fuel. 73(1994) 1855-1857. https://doi.org/10.1016/0016-2361(94)90211-9.

[3] A.R.K. Gollakota, A review on hydrothermal liquefaction of biomass, Renew. Sustain. Energy Rev. 81 (2018) 1378–1392. https://doi.org/10.1016/j.rser.2017.05.178.

[4] R. Bounaceur, Modélisation cinétique de l'évolution thermique des pétroles dans les gisements, PhD Thesis (in french), Vandoeuvre-les-Nancy, INPL, 2001. http://www.theses.fr/2001INPL002N (accessed September 5, 2019).

[5] L. Xu, Assessment of a dry and a wet route for the production of biofuels from microalgae: Energy balance analysis, Bioresour. Technol. 102 (2011) 5113–5122. https://doi.org/10.1016/j.biortech.2011.01.066.

[6] U. Jena, K.C. Das, Comparative Evaluation of Thermochemical Liquefaction and Pyrolysis for Bio-Oil Production from Microalgae, Energy Fuels. 25 (2011) 5472–5482. https://doi.org/10.1021/ef201373m.

[7] S.M. Heilmann, H.T. Davis, L.R. Jader, P.A. Lefebvre, M.J. Sadowsky, F.J. Schendel, M.G. von Keitz, K.J. Valentas, Hydrothermal carbonization of microalgae, Biomass Bioenergy. 34 (2010) 875–882. https://doi.org/10.1016/j.biombioe.2010.01.032.

[8] M. Audo, M. Paraschiv, C. Queffélec, I. Louvet, J. Hémez, F. Fayon, O. Lépine, J. Legrand, M. Tazerout, E. Chailleux, B. Bujoli, Subcritical Hydrothermal Liquefaction of

Microalgae Residues as a Green Route to Alternative Road Binders, ACS Sustain. Chem. Eng. 3 (2015) 583–590. https://doi.org/10.1021/acssuschemeng.5b00088.

[9] I. Borghol, C. Queffélec, P. Bolle, J. Descamps, C. Lombard, O. Lépine, D. Kucma, C. Lorentz, D. Laurenti, V. Montouillout, E. Chailleux, B. Bujoli, Biosourced analogs of elastomer-containing bitumen through hydrothermal liquefaction of Spirulina sp. microalgae residues, Green Chem. 20 (2018) 2337–2344. https://doi.org/10.1039/C8GC00094H.

[10] E. Chailleux, M. Audo, B. Bujoli, C. Queffelec, J. Legrand, M. Paraschiv, M. Tazerout, O. Lepine, Viscoelastic Material Produced by hydrothermal liquefaction of microalgae, Patent WO2015044891.https://patentscope.wipo.int/search/en/detail.jsf?docId=WO2015044891 (accessed February 19, 2020).

[11] M. Pecchi, F. Patuzzi, D. Basso, M. Baratieri, Enthalpy change during hydrothermal carbonization of biomass: a critical review, J. Therm. Anal. Calorim. (2019). https://doi.org/10.1007/s10973-019-09117-4.

[12] M. Pecchi, F. Patuzzi, V. Benedetti, R. Di Maggio, M. Baratieri, Thermodynamics of hydrothermal carbonization: Assessment of the heat release profile and process enthalpy change, Fuel Process. Technol. 197 (2020) 106206. https://doi.org/10.1016/j.fuproc.2019.106206.

[13] A. Funke, F. Ziegler, Heat of reaction measurements for hydrothermal carbonization of biomass., Bioresour. Technol. 102 (2011) 7595–7598. https://doi.org/10.1016/j.biortech.2011.05.016.

[14] F. Merzari, Hydrothermal Carbonization of Biomass Design of a Bench-Scale Reactor for Evaluating the Heat of Reaction.pdf, (2018).

[15] E.G. Bligh, W.J. Dyer, A Rapid Method of Total Lipid Extraction and Purification, Can. J. Biochem. Physiol. 37 (1959) 911–917. https://doi.org/10.1139/o59-099.

[16] J. Folch, M. Lees, G.H. Sloane Stanley, A simple method for the isolation and purification of total lipides from animal tissues, J. Biol. Chem. 226 (1957) 497–509.

[17] O.H. Lowry, N.J. Rosebrough, A.L. Farr, R.J. Randall, Protein measurement with the Folin phenol reagent, J. Biol. Chem. 193 (1951) 265–275.

[18] M. DuBois, K. A. Gilles, J. K. Hamilton, P. A. Rebers, and F. Smith, Colorimetric Method for Determination of Sugars and Related Substances, Analytical Chemistry. 28 (1956) 350-356. https://doi.org/10.1021/ac60111a017.

[19] ThermExcel Tables Physical characteristics of boiling water, Boiling water, Density, Specific enthalpy, sensible heat, absolute, atmospheric, gauge pression, point, (n.d.). https://www.thermexcel.com/english/tables/eaubou1.htm (accessed September 18, 2019).

[20] Dortmund Data Bank, Vapor Pressure Calculation by Antoine Equation (Water). http://ddbonline.ddbst.de/AntoineCalculation/AntoineCalculationCGI.exe?component=Water (accessed September 18, 2019).

[21] K. Anastasakis, P. Biller, R.B. Madsen, M. Glasius, I. Johannsen, Continuous Hydrothermal Liquefaction of Biomass in a Novel Pilot Plant with Heat Recovery and Hydraulic Oscillation, Energies. 11 (2018) 2695. https://doi.org/10.3390/en11102695.